https://doi.org/10.22226/2410-3535-2023-2-126-131

Check for updates

Effect of high-dense electropulsing with different energies on the structure and strength of nickel cryorolled to different strains

M. V. Markushev†, I. Sh. Valeev, E. V. Avtokratova, R. R. Ilyasov, A. Kh. Valeeva, S. V. Krimsky, O. Sh. Sitdikov

Institute for Metals Superplasticity Problems, RAS, Ufa, 450001, Russia

†mvmark@imsp.ru

The effect of thermomechanical treatment, based on combination of isothermal cryorolling at liquid nitrogen temperature to strains ranging from 30 to 90% and subsequent single electric pulsing with an integral current density K_j up to 1.6×10^4 A^{2}s/mm^4, on the structure and hardness of an initially coarse-grained pure nickel was studied. It is shown that the considered treatment is quite a powerful method to control the Ni structure and strength through grain and grain boundary design. The right chose of conditions of cryogenic straining and electro-heat action give ability to high efficient production of abnormally and partially work-hardened sheets with light tuning of crystallite size and fractions of recrystallized grains and high angle boundaries, in particular, the fine-grained sheet with a grain size of about 3 μm and 50% fraction of the twin boundaries.

Keywords: nickel, cryorolling, high-dense electropulsing, structure, strength.

1. Introduction

Enhancing the service properties of metals and alloys through deep grain refinement is a topic area of modern materials science [1,2]. Thermomechanical treatment (TMT) based on severe plastic deformation (SPD) (to true strains $e>1$) [3–7], especially implemented at cryogenic temperatures, is currently considered as one of the potential industrial methods to achieve the goal [8–14], in particular, via processing of an ultrafine grained (UFG) structure (grain size <10 μm). However, few studies had shown that UFG structure did not formed in some severely cryodeformed pure metals and solid solutions. For instance, in pure Al [15], Al alloys [16–19], Ni [20] and Cu [21,22]. As for Ni, isothermal rolling at a temperature of liquid nitrogen in the range of $e=0.3-2.3$ [20] resulted in the development of nanocellular substructure inside of coarse fibers and an extremely low amount of dynamically recrystallized fine grains only. Meanwhile, such a structure provides an almost 3-fold increase in hardness, being much higher than at room temperature rolling, resulting in formation of partially recrystallized structure [23]. Thus, it could be concluded that the strong suppression of dynamic recovery and dynamic recrystallization under cryostraining with the predominant processing of dislocation/cellular structure, could be an effective way for metals and alloys strengthening.

Nevertheless, it was found [14,24–26] that TMT involving cryorolling and subsequent high-dense electric pulsing (HDEP) ensured the formation of the UFG structure in a number of metallic materials. The cause is that the heat/current treatment played a crucial role in activation of the static recovery and recrystallization of the initial highly work-hardened material, allowing grain refinement to be enhanced due to the ultra-fast heating, increasing the number of recrystallization centers, and the extremely short annealing time, that limits grain growth [27–31]. Owing to the low UFG structure stability, such TMT is much important to process pure metals and solid solutions.

The aim of the present study was to evaluate the effect of TMT, involving isothermal rolling at a temperature of liquid nitrogen to different strains and further HDEP with different energies, on the structuring and strengthening/softening of pure Ni.

2. Material and methods

The starting material — coarse-grained pure Ni, was initially cryorolled with reductions in the range of $e=0.3-2.3$ (30–90%) (more details of processing are described in [20]). Further HDEP was performed on flat dog-bone shaped specimens with a thickness of 0.4 mm and gauge dimensions of 3×4 mm^2. The specimens were cut out along the rolling direction and treated in massive current connectors. The temperature of heating of the gauge part was followed from:

$$S(T_C)=\int_{T_1}^{T_C}\rho c\sigma_e dT,\quad K_j=\int_0^{\tau}j^2dt,\quad S(T)=K_j,$$

where T_C is the calculated temperature, T_1 is the reference temperature of the sample, τ is the duration of the electric impulse. For the selected current parameters (current intensity, K_j, from 1.1×10^4 to 1.6×10^4 A^2 s/mm^4), the temperature interval of sample heating was within 300 and 670°C. At an impulse time of about 10^{-4} s and a frequency of current 10^4 Hz, the depth of its penetration inside the sample was about 0.2 mm [27]. This means that the skin-effect in

the samples used was absent suggesting a uniform current distribution in the gauge part.

The microstructure of Ni was analyzed in the rolling plane using a TESCAN MIRA 3 LMH scanning electron microscope (SEM), equipped with EBSD analyzer and HKL Channel 5 software. X-ray diffraction analysis was performed on a DRON-4-07 diffractometer in Cu-Kα radiation at a voltage of 40 kV and a current of 30 mA with a wavelength λ=1.54418 Å. Microhardness of Ni was determined by the Vickers method on an MVDM 8 "AFFRY" digital tester at a load of 0.5 N and a time of 10 sec (see more details in [20]).

3. Results and discussions

Recall that in [20] the dislocation/cellular structures were formed in coarse-grained pure Ni regardless of the cryrolling strain. Even after rolling to 90% the structure consisted of cells, dense dislocation walls, and (micro) shear bands, represented a network of low-angle boundaries (LABs) with a fraction of high-angle boundaries (HABs) of only about 5%. Figure 1 and Table 1 illustrate the structure parameters obtained by further HDEP. In the metal rolled with 30%, the effect of electropulsing was insignificant (Fig. 1a – c, Table 1). Sense structural changes start at the dislocation level with activation of static recovery. However, the transformations of dislocation structures involving annihilation of individual dislocations were not so intense and uncompleted within a short time of current action at HDEP over the entire temperature (energy) range studied. This was associated with a low accumulated strain energy resulting from rather low levels of the integral dislocation density and lattice distortion (Table 1). Meanwhile, the static recrystallization was also not so active even after the pulsing with maximum energy and detected in the form of nucleus of individual grains in the regions, adjacent to the original grain boundaries and triple junctions (Fig. 1c). Thus, the Ni structure remained mostly work-hardened with an increased dislocation density and stored energy (Fig. 1c, Table 1) even after the pulsing with the heating temperature above 600°C, being of $0.4T_m$ — melting point.

A bit different, but quite similar, HDEP behavior was found in Ni rolled to 50 and 70% (Fig. 1d – i). At low impulse energies the deformation structures were relatively stable (Fig. 1d, g), as in the less strained state (see Fig. 1a, b). However, a pulsing with K_j=1.3×10^4 A^2 s/mm^4 activated static recrystallization with frequent formation of arrays of fine recrystallized grains between and within elongated fragments of the original grains (Fig. 1e, h). Increasing the pulse energy to the maximum value led to the occurrence of recrystallization practically in the entire sample volume (Fig. 1f, i) and to the formation of a fairly homogeneous fine grain structure with grain size in the range of 3 – 6 μm (Fig. 1, Table 1).

As might be expected, the HDEP impulse of minimum capacity was required to obtain the UFG structure in Ni cryodeformed to the maximum strain. And an almost completely recrystallized UFG structure with a minimum grain size of about 3 μm was processed in the 90% rolled metal after the pulsing even with K_j= 1.1×10^4 A^2 s/mm^4 (Fig. 1j). Therewith, after cryorolling to high strains (70 – 90%) the grain size roughly corresponded to the subgrain size, while it was up to 4 times larger after lower reductions. This can be explained by the predominance of discontinuous static recrystallization after low strain and a gradual increase in the contribution of continuous ("*in situ*") one with increasing pre-strain [1]. Meanwhile, the increase in HDEP energy, as also expected, led to grain coarsening through normal grain growth to about 6 μm (Fig. 1k, l and Table 1).

As can be seen in Fig. 2, despite the strong suppression of dynamic recrystallization, Ni was more than doubly continuously hardened by dislocation/substructure strengthening due to cryorolling. And the highest effect was realized at 30% straining. In contrast, the effect of further HDEP, leading to Ni softening, was strongly pronounced in the states rolled to strains above 30%. However, the dependences

Table 1. Parameters of structure of cryorolled and HDEP processed Ni: d_{sg} and d_g — subgrain and grain size, D — coherent domain size, Θ — mean misorientation angle of boundaries; F_{rec}, F_{HABs}, F_Σ — fractions of recrystallized grains, high-angle and twin boundaries; $\langle\varepsilon^{1/2}\rangle$ — mean square microstrain of the crystal lattice.

Strain, %	K_j, 10^4 A^2 s/mm^4	T_c, °C	d_{sg}, μm	d_g, μm	F_{rec}, %	Θ, deg	F_{HABs}, %	$F_{\Sigma3+\Sigma9}$, %	$F_{\Sigma3\ldots\Sigma49}$, %	Dislocation density 10^{13} m^{-2}	D, nm	$\langle\varepsilon^{1/2}\rangle$, %
30	0	20	0.3	-	0	7	7	<1	<1	9	152 ± 3	0.094 ± 0.003
	1.1	320	1.7	-	<1	6	6	<1	<1	8	121 ± 2	0.067 ± 0.001
	1.3	430	1.6	-	<1	15	24	2	2	6	135 ± 4	0.057 ± 0.001
	1.6	670	1.5	6.2	5	10	13	1	2	5	138 ± 3	0.048 ± 0.001
50	0	20	0.3	2.9	1	5	4	<1	<1	24	75 ± 2	0.126 ± 0.003
	1.1	320	1.8	-	<1	7	8	<1	<1	20	65 ± 2	0.092 ± 0.001
	1.3	430	2.0	4.0	16	31	59	10	11	12	72 ± 3	0.063 ± 0.001
	1.6	670	6.4	8.0	94	49	94	34	38	7	85 ± 4	0.048 ± 0.001
70	0	20	0.2	3.3	3	6	5	<1	<1	30	72 ± 4	0.121 ± 0.005
	1.1	320	1.4	-	<1	4	2	<1	<1	22	77 ± 2	0.118 ± 0.001
	1.3	430	1.4	3.3	26	18	32	7	8	12	95 ± 3	0.082 ± 0.001
	1.6	670	5.5	6.4	95	49	93	35	39	<1	117 ± 4	0.001 ± 0.001
90	0	20	0.2	2.5	3	7	7	<1	<1	35	68 ± 4	0.165 ± 0.002
	1.1	320	2.8	3.2	92	47	92	44	50	<1	129 ± 2	0.001 ± 0.001
	1.3	430	3.2	4.5	85	45	84	42	46	<1	134 ± 2	0.001 ± 0.001
	1.6	670	4.4	4.7	95	48	92	41	46	<1	141 ± 2	0.001 ± 0.001

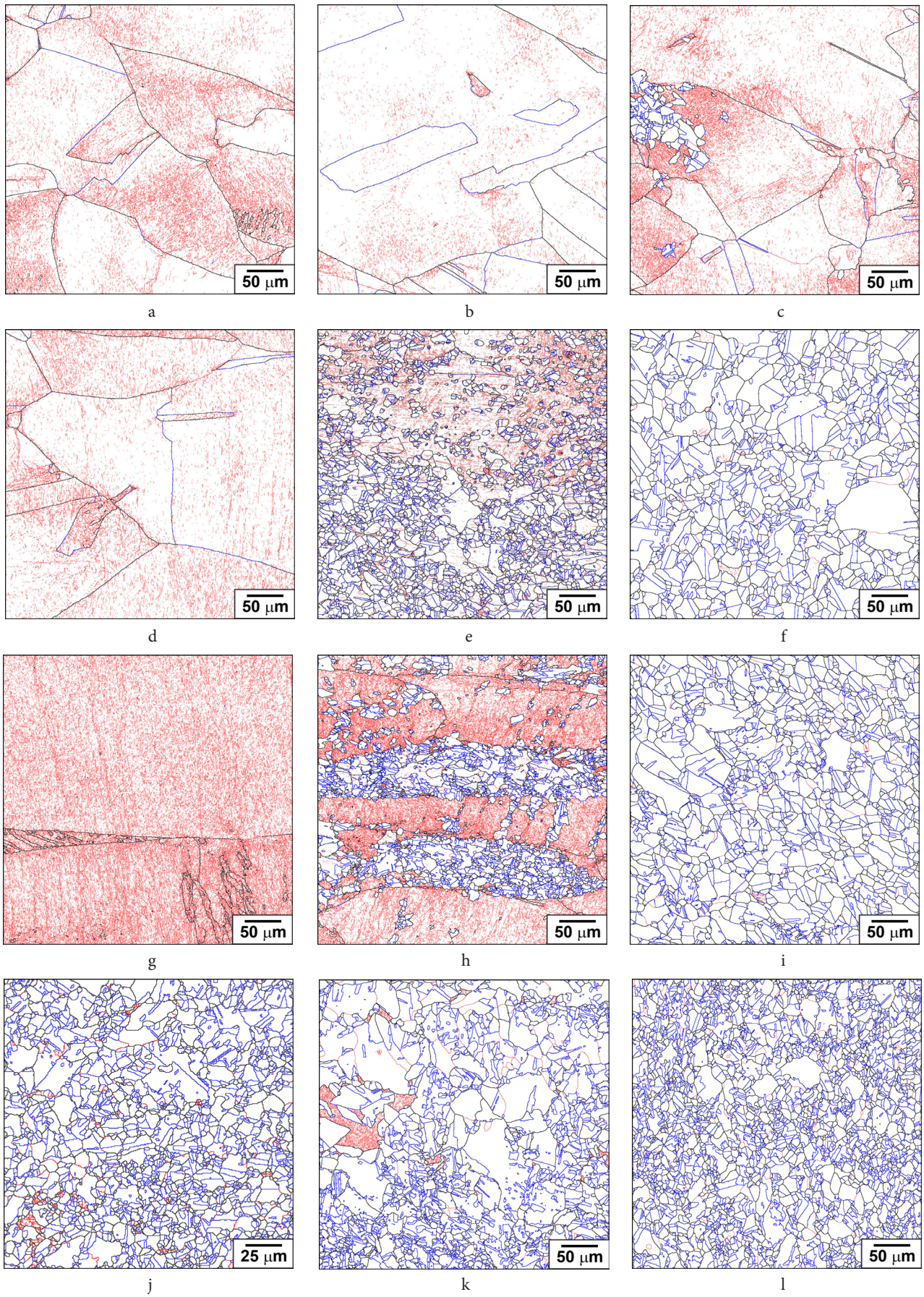

Fig. 1. (Color online) SEM-EBSD reconstructed structures of Ni cryorolled to 30 (a – c), 50 (d – f), 70 (g – i) and 90% (j – l) and further HDEP treated with integral current density (K_j) 1.1×10^4 $A^2 s/mm^4$ (a, d, g, j), 1.3×10^4 $A^2 s/mm^4$ (b, e, h, k) and 1.6×10^4 $A^2 s/mm^4$ (c, f, i, l). Here and after, low- and high-angle boundaries indicated by red and black lines, consequently, and twin- boundaries indicated by blue lines. Note the differed scale in (j).

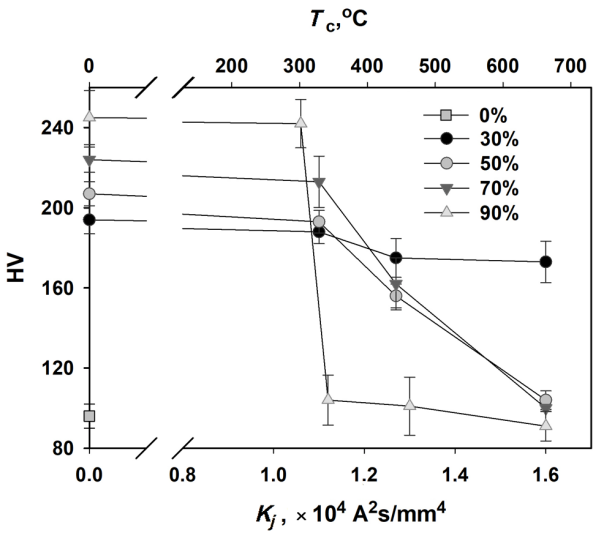

Fig. 2. Microhardness (HV) of starting (0%) and cryorolled to 30, 50, 70 and 90% strains Ni vs current intensity (K_j) of further HDEP.

of their hardness on the pulsing energy were of a similar nature. In particular, in the area of low energies, the hardness remains close to that achieved during rolling. This means the existence of a power (temperature) interval of stability of deformation structures at HDEP. The sense decrease in hardness is observed when a certain "threshold" value of K_j is exceeded. Therewith, the higher was the pre-strain, the faster was the metal softening. Thus, these data confirm the well-known tendency for annealing the work-hardened metal: as usual, softening, activated by HDEP, begins at a pulsing energy directly proportional to the amount of cryostraining (stored energy).

Besides, the intensity of softening was higher in the strongly work-hardened state. That is, the higher the strain, the faster, and at lower impulse energy, the loss of hardness to values corresponding to the undeformed material took place. Consequently, after rolling with 90% reduction, this loss occurred in the narrowest range of HDEP energy. With further increase of impulse energy, the hardness decrease was insignificant because of control by the normal growth of recrystallized grains (Table 1). The behavior was also expectable because after static recrystallization, during which structural (dislocation) hardening was lost, there was commonly observed the following growth of new grains, which should lead to additional softening of the nickel due to the some loss of grain boundary strengthening effect (Hall-Petch strengthening) caused by grain coarsening. And the less intense softening of the Ni rolled to 50 and 70% was controlled by the incompleteness of static recrystallization (Fig. 1).

The HDEP behavior of the Ni after rolling to 30% was of particular interest, because a fairly long and less intense interval of hardness loss was found (Fig. 2). Apparently, it was due to structural transformations during HDEP discussed above. As noted, the main distinction in the structures found after HDEP was the absence of statically recrystallized grains in this condition. This means that its structural transformations were controlled by static recovery, which by its nature requires less driving force than recrystallization. As a result, the Ni hardness achieved by cryorolling remained relatively stable even after exposure to high-energy electric impulses.

Another interesting point detected in [20] for the cryodeformed Ni was the absence of deformation twinning even under straining to 90%. The negligible fraction of twin boundaries was also observed in the HDEP-ed samples with energies below the threshold K_j values (Fig. 3 a, b), when the transformation of the deformation structure was controlled by static recovery. In this case, the fraction of special

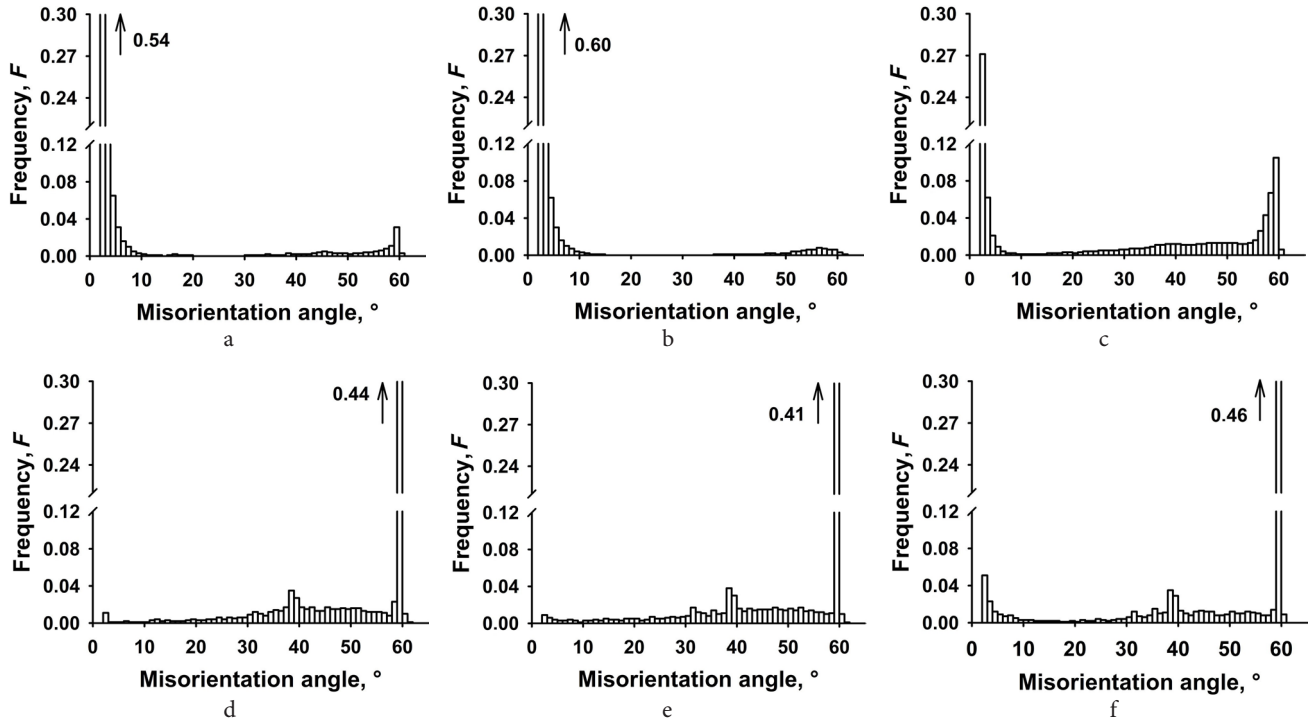

Fig. 3. Boundary spectra of Ni cryorolled to 30 (a), 50 (b, c, d) and 90% (e, f) and further HDEP treated with integral current density (K_j) 1.10×10^4 A² s/mm⁴ (a, b, e), 1.3×10^4 A² s/mm⁴ (c, f) and 1.6×10^4 A² s/mm⁴ (d).

boundaries formed the weak peaks on the distributions, virtually by the fragments of the original annealing twins that survived at high straining and further pulsing. However, intense formation of the first-order annealing twin boundaries with Σ3 (with misorientation angles close to 60°) occurred practically simultaneously with the formation of centers of static recrystallization (see Fig. 3 c, d, e). At the final stage of recrystallization (at HDEP with high K_j values) twin boundaries of the second order with Σ9 forming peaks at misorientation angles close to 38° were also detected (Fig. 3 d, f and Table 1). As a result, the finest structure with the grain size of about 3 μm, obtained after cryorolling to 90% and subsequent HDEP with K_j=1.1×10⁴ A² s/mm⁴ (Figs. 1j, 3 e and Table 1), has the fraction of twin boundaries of the first and second orders (Σ3 + Σ9) of about 44% and the total fraction of special boundaries (Σ from 3 to 49) of about 50%. If these data are compared with those after a half-hour furnace annealing at the corresponding temperature of 300°C, the similarly rolled nickel (Fig. 4) exhibited more than twice as large grains (≈7 μm) with about half the corresponding fractions of twin boundaries — 26 and 29%, respectively.

It is known [32] that formation of annealing twins due to growth accidents upon static recrystallization is a common phenomenon of work-hardened cubic materials with dense packing, such as austenitic iron, alpha brass, copper, and nickel. It is also well reported [for instance, 33 – 35] the importance of simultaneous processing the structure with finer grains and a higher fraction of special boundaries to improve their mechanical properties. The reason is that the twin boundaries are quite effective to restrict dislocation motion and thus to act as stabilizing interfaces for materials strengthening. Besides, increase in homogeneity of microstructure and proportion of low-R coincidence site lattice boundaries enhances the Ni fracture toughness [36]. Moreover, in [37] there was shown the Ni corrosion resistance increase with fraction of nanoscale twins, which is much important for nuclear steam generator pipes.

Based on the data presented in [33 – 37] and obtained in the study it can be concluded that TMT involving a combination of severe plastic deformation at cryogenic temperatures and subsequent HDEP could be an effective way to process products out of pure metals and solid solutions with controlled parameters of ultrafine grain structure and mechanical behavior. Such a structure will undoubtedly make it possible to obtain constructions with enhanced physical, chemical and mechanical properties. And, most importantly, to improve the parameters that limit their industrial applications, such as operating temperature and stress, as well as the aggressiveness of environment, which largely determined by the dispersity of crystallites and the proportion of their special (low-energy) boundaries actively preventing their failure.

Conclusions

1. Low-energy high-dense electric pulsing with K_j<1.1×10⁴ A² s/mm⁴ of pure Ni cryorolled to various strains resulted in insignificant changes in its strength. Activation of the static recovery mainly led to improvement of the deformation structure, which is characterized by some decrease in internal stresses and dislocation density, as well as to slight increase in the crystallite size, average angle of misorientation of the boundaries and the fraction of high-angle boundaries.

2. Exceeding a certain "threshold" level of pulse energy in nickel pre-rolled to reductions of more than 30% activated static recrystallization, realizing the nucleation and limited growth of new grains. Such structural changes were accompanied by a sharp decrease in internal stresses, dislocation density and an increase in the angular parameters of the grain structure, which led to a rapid loss of metal hardness. The higher the rolling strain, the narrower the pulsing interval ensuring intense softening. A further increase in HDEP energy led to the normal growth of new grains, as well as to the stabilization of the strength at the level of starting soft metal.

3. Completely recrystallized structure with a grain size of 3 to 7 μm can be obtained by HDEP in cryorolled pure Ni. The formation of such a structure was conditioned by the development of a large number of annealing twins due to static recrystallization, forming a network of high-angle boundaries with a fraction of Σ3…Σ49 special boundaries up to 50%.

4. It was found an effective method to control the structure and properties of fcc pure metals like Ni by grain and grain boundary design based on combination of cryogenic straining and subsequent high-dense electric pulsing.

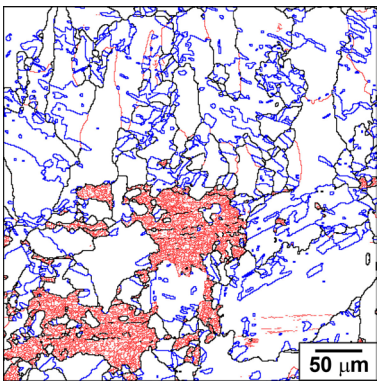

a

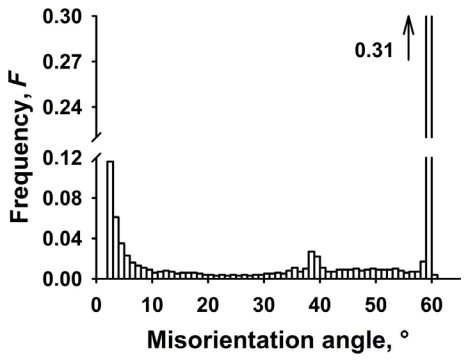

b

Fig. 4. (Color online) SEM-EBSD reconstructed structure of Ni cryorolled to 90% and further annealed during 30 min at 300°C (d_g = 7 μm, F_{rec} = 59%, $F_{\Sigma3+\Sigma9}$ = 26%). EBSD map (a), boundary spectrum (b).

Acknowledgements. The work was supported by the Ministry of Science and Higher Education of Russian Federation through the state assignment of IMSP RAS. It was performed using the facilities of the shared services center "Structural and Physics-Mechanical Studies of Materials" at the Institute for Metals Superplasticity Problems of Russian Academy of Sciences.

References

1. F. J. Humphreys, M. Hatherly. Recrystallization and Related Annealing Phenomena, 2nd ed. Amsterdam, Elsevier (2004) 658 p. Crossref
2. V. I. Yelagin. Light Alloy Technology. 2, 6 (2008). (in Russian)
3. R. Z. Valiev, I. V. Aleksandrov. Bulk Nanostructured Metallic Materials: Processing, Structure, and Properties. Moscow, Akademkniga (2007) 398 p. (in Russian)
4. R. R. Mulyukov, R. M. Imayev, A. A. Nazarov, M. F. Imayev, V. M. Imayev. Superplasticity of Ultrafine Grained Alloys: Experiment, Theory, Technologies. Moscow, Nauka (2014) 284 p. (in Russian)
5. V. M. Segal, V. I. Reznikov, V. I. Kopylov et al. Processes of Metal Structure Formation upon Plastic Deformation. Minsk, Science and Technology (1994) 232 p. (in Russian)
6. K. Edalati, A. Bachmaier, V. A. Beloshenko, Y. Beygelzimer, V. D. Blank, W. J. Botta, et al. Mater. Res. Lett. 10 (4), 163 (2022). Crossref
7. E. Avtokratova, O. Sitdikov, M. Markushev, M. Linderov, D. Merson, A. Vinogradov. Mater. Sci. Eng. A. 806, 140818 (2021). Crossref
8. E. Ma. JOM. 58 (4), 49 (2006). Crossref
9. J. Yin, J. Lu, H. Ma, P. Zhang. J. Mater. Sci. 39, 2851 (2004). Crossref
10. B. Y.-H. Zhao, X.-Z. Liao, S. Cheng, E. Ma, Y. T. Zhu. Adv. Mater. 18, 2280 (2006). Crossref
11. Y. Huang, P. B. Prangnell. Acta Mater. 56, 1619 (2008). Crossref
12. T. Konkova, S. Mironov, A. Korznikov, S. L. Semiatin. Acta Mater. 58, 5262 (2010). Crossref
13. D. C. C. Magalhães, A. M. Kliauga, M. Ferrante, V. L. Sordi. J Mater. Sci. 52, 7466 (2017). Crossref
14. S. Krymskiy, O. Sitdikov, E. Avtokratova, M. Markushev. Trans. Nonfer. Met. Soc. of China (English Edition). 30 (1), 14 (2020). Crossref
15. I. Sh. Valeev, A. Kh. Valeeva, R. R. Ilyasov, E. V. Avtokratova, S. V. Krimsky, O. Sh. Sitdikov, M. V. Markushev. Lett. Mater. 11 (3), 351 (2021). (in Russian) Crossref
16. T. Shanmugasundaram, B. S. Murty, V. Subramanya Sarma. Proc. Int. Conf. on Advanced Materials and Composites (ICAMC-2007). Oct 24 – 26, Trivandrum, (2007) p. 577.
17. S. Cheng, Y. H. Zhao, Y. T. Zhu, E. Ma. Acta Mater. 55, 5822 (2007). Crossref
18. H. R. Song, Y. S. Kim, W. J. Nam. Met. Mat. Int. 12 (1), 7 (2006). Crossref
19. Y. B. Lee, D. H. Shin, W. J. Nam. Met. Mat. Int. 10 (5), 407 (2004). Crossref
20. M. V. Markushev, I. Sh. Valeev, E. V. Avtokratova, R. R. Ilyasov, A. Kh. Valeeva, S. V. Krimsky, O. Sh. Sitdikov. Lett. Mater. 12 (4s), 409 (2022). Crossref
21. M. Markushev, I. Valeev, A. Valeeva, R. Ilyasov, E. Avtokratova, S. Krymskiy, O. Sitdikov. FACTA UNIVERSITATIS. Series: Mechanical Engineering. 2022. (online first) Crossref
22. P. A. Khaimovich. Prob. Atomic Sci. Technology. 4, 28 (2006). (in Russian)
23. I. S. Valeev, A. K. Valeeva, R. R. Ilyasov, O. S. Sitdikov, M. V. Markushev. Lett. Mater. 9 (4), 447 (2019). Crossref
24. T. Konkova, I. Valeev, S. Mironov, A. Korznikov, M. M. Myshlyaev, S. L. Semiatin. J. Mater. Res. 29 (22), 2727 (2014). Crossref
25. T. Konkova, I. Valeev, S. Mironov, A. Korznikov, G. Korznikova, M. M. Myshlyaev, S. L. Semiatin. J. All. Comp. 659, 184 (2016). Crossref
26. M. V. Markushev, R. R. Ilyasov, S. V. Krymskiy, I. S. Valeev, O. S. Sitdikov. Lett. Mater. 11 (4), 491 (2021). (in Russian) Crossref
27. H. Knoepfel. Pulsed High Magnetic Fields. Amsterdam, North-Holland (1970) 392 p.
28. H. Conrad, N. Karam, S. Mannan. Scr. Metall. 17 (3), 411 (1983). Crossref
29. H. Conrad, A. F. Sprecher, W. D. Cao, X. P. Lu. JOM. 42, 28 (1990). Crossref
30. Y. Sheng, Y. Hua, X. Wang, X. Zhao, L. Chen, H. Zhou, J. Wang, C. C. Berndt, W. Li. Materials. 11 (2), 185 (2018). Crossref
31. Yu. V. Baranov, O. A. Troitsky, Yu. S. Avramov, A. D. Shlyapin. Physical fundamentals of electropulse and electroplastic treatments and new materials. Moscow, MSIU (2001) 844 p. (in Russian)
32. R. W. Cahn, P. Haasen. Physical Metallurgy, 4th ed. North Holland (1996) 897 p.
33. Z. Cheng, H. Zhou, Q. Lu, H. Gao, L. Lu. Science. 362, 559 (2018). Crossref
34. L. Lu, Y. Shen, X. Chen, L. Qian, K. Lu. Science. 304, 422 (2004). Crossref
35. F. H. Duan, Y. Lin, Q. Li, J. H. Luan, J. Lu, J. Pan, Y. Li. J. Mat. Sci. Tech. 137, 123 (2023). Crossref
36. S. Kobayashi, T. Maruyama, S. Tsurekawa, T. Watanabe. Acta Mater. 60, 6200 (2012). Crossref
37. G. Meng, Y. Shao, T. Zhang, Y. Zhang, F. Wang. Electrochimica Acta. 53, 5923 (2008). Crossref